NASA CONTRACTOR
REPORT

NASA CR-183653

NAS8-35918

A TWO-LAYER MULTIPLE-TIME-SCALE TURBULENCE MODEL AND GRID INDEPENDENCE STUDY

By S. -W. Kim
Universities Space Research Association
4950 Corporate Drive, Suite 100
Huntsville, Alabama 35806

and

C. -P. Chen
Department of Mechanical Engineering
University of Alabama in Huntsville
Huntsville, Alabama 35899

March 1989

Final Report

Prepared for
NASA, George C. Marshall Space Flight Center
Marshall Space Flight Center, Alabama 35812

ACKNOWLEDGMENT

This work has been supported, in part, by NASA contract NAS8-35918.

TABLE OF CONTENTS

LIST OF ILLUSTRATIONS

CONTRACTOR REPORT

A TWO-LAYER MULTIPLE-TIME-SCALE TURBULENCE MODEL AND GRID INDEPENDENCE STUDY

INTRODUCTION

For wall bounded turbulent boundary layer flows, the logarithmic velocity profile prevails almost universally throughout the thin shear layer. The wall function method is based on the validity of the logarithmic velocity profile and the local equilibrium condition (the generation rate is almost equal to the dissipation rate of the turbulent kinetic energy) of turbulence. The wall function method lost its validity in many instances (i.e., separated flows, turbulent boundary layer flows subjected to strong adverse pressure gradient, and transition flows for which the local turbulent Reynolds number is sufficiently low). Nevertheless, partly due to the consideration of computational efficiency and partly due to the difficulty in developing and implementing the low Reynolds number turbulence models for elliptic flows, the wall function method has been used dominantly even for separated and recirculating flows. The appropriateness of the wall function method began to be re-evaluated [1], and a number of two-layer turbulence models [2-5] and a number of low Reynolds number turbulence models [6,7] began to appear in recent years. A comparative study on various low Reynolds number turbulence models can be found in Reference 7.

In the simplest form of the two-layer turbulence models, the turbulent eddy viscosity inside the near-wall, low turbulent Reynolds number layer is expressed using the mixing length theory which is based on the Kolmogorov-Prandtl theory [8] of turbulence. A few flow cases in which the simplest form two-layer model yielded significantly improved computational results over the wall function method can be found in Reference 1. The two-layer turbulence model presented in this report belongs to the simplest class of two-layer models in a sense that the mixing length assumption has been used to derive the turbulent eddy viscosity expression for the near wall low turbulent Reynolds number region.

In some of the finite element computation of turbulent flows [9-11], the tangential velocity has been evaluated using the wall function method and the vanishing normal velocity has been prescribed at the near wall boundary. Use of the vanishing normal velocity at the near wall boundary has been justified based on the assumption that the magnitude of the normal velocity would be vanishingly small. However, it brought about an uncertainty with regard to satisfying the conservation of mass equation, since the flow below the near wall boundary (the viscous sublayer and the transition region) may accelerate or decelerate depending on the pressure distribution in the region, and accordingly, the normal velocity component may seldom vanish. Slightly different implementations of the wall function method to satisfy the conservation of mass constraint more rigorously can be found in References 12 and 13. In Reference 12, the normal velocity at the near wall boundary has been evaluated by integrating the conservation of mass equation in the region below the near wall boundary; and in Reference 13, the normal velocity at the near wall boundary has been estimated using an analytical expression obtained from a near-wall analysis based on mixing length theory with the pressure gradient effect excluded. Implementation of such methodologies for three-dimensional flows may be complicated or exceedingly difficult. In many finite difference methods, the difficulty of satisfying the conservation of mass equation has been circumvented by using the staggered grids [14].

In the two-layer model presented herein, the computational domain for the flow equations penetrated up to the wall, where no-slip boundary condition has been prescribed. Use of the two-layer model in a finite element computation of turbulent flows partly eliminated an uncertainty involved in satisfying the conservation of mass constraint. Grid independence study has been made for the near-wall layer; and the computational results have been compared with the experimental data as well as those obtained by using the wall function method. The purpose of the present study has also been to clarify the uncertainty in satisfying the conservation of mass equation, which has been caused by using the vanishing normal velocity in the context of the wall function method, by comparing the computational results obtained by using the two-layer model with those obtianed by using the wall function method.

In finite difference methods, it is known that a significant amount of grid points are required inside the near-wall layer. Discussion on computational efficiency, in comparison with the finite difference methods, is also included.

NEAR WALL EDDY VISCOSITY EQUATION FOR TWO-LAYER MODEL

Very close to the wall, inside the viscous sublayer, the eddy viscosity grows in proportion to the cubic power of distance from the wall and the mean tangential velocity varies in proportion to the same wall distance. The eddy viscosity equation given below has been derived by incorporating these experimentally observed behavior of turbulence into the logarithmic velocity profile equation, and the modified logarithmic velocity profile equation has been derived by integrating the eddy viscosity equation. Detailed derivation of these equations are given in Reference 15.

$$\nu_t^+ = \frac{1}{\kappa} E \{\exp(\kappa u^+) - [1 + (\kappa u^+) + \frac{1}{2}(\kappa u^+)^2]\} \tag{1}$$

$$y^+ = u^+ + \frac{1}{E} \{\exp(\kappa u^+) - [1 + (\kappa u^+) + \frac{1}{2}(\kappa u^+)^2 + \frac{1}{6}(\kappa u^+)^3]\} \tag{2}$$

where ν_t^+ ($\nu_t^+ = \nu_t/\nu$) is a non-dimensional turbulent eddy viscosity; ν_t is the turbulent eddy viscosity; ν is the kinematic viscosity of the fluid; u^+ ($u^+ = u/u_\tau$) is a non-dimensional velocity; u_τ [$u_\tau = \sqrt{(\tau_w/\rho)}$] is the wall friction velocity; τ_w is the wall shearing stress; y^+ ($y^+ = u_\tau y/\nu$) is the wall coordinate; κ is the von Karmann constant; and E is an experimentally determined constant coefficient. The values of κ and E used in Reference 15 are given as 0.4 and 7.7, respectively; whereas in most of numerical analysis of turbulent flows using the k-ε type turbulence models, κ = 4.1 and E = 9 have been used. The eddy viscosity and the modified logarithmic velocity profiles obtained by using these two different sets of coefficients are compared with experimental data in Figures 1 and 2. It can be seen that these two sets of coefficients yielded almost identical results. In the present study, κ = 4.1 and E = 9 have been used throughout.

HIGH REYNOLDS NUMBER TURBULENT BOUNDARY LAYER FLOW EQUATIONS

The turbulent boundary layer flow equations and the high turbulent Reynolds number multiple-time-scale turbulence model are described briefly below for completeness. Details on the turbulence model can be found in Reference 11.

The turbulent boundary layer flow equations are given as:

$$\frac{\partial u}{\partial x} + \frac{\partial v}{\partial y} = 0 \tag{3}$$

$$u \frac{\partial u}{\partial x} + v \frac{\partial u}{\partial y} - \frac{\partial}{\partial y} [(\nu + \nu_t) \frac{\partial u}{\partial y}] = - \frac{dp}{dx} \tag{4}$$

where u and v are the time averaged mean velocities in flow direction and in transverse direction, respectively, and p is the pressure. The turbulent eddy viscosity inside the near-wall layer for the mean momentum equation has been computed by using equation (1). The turbulent eddy viscosity outside the near-wall layer has been obtained by using the eddy viscosity equation given as [11],

$$\nu_t = c_{\mu f} \frac{k^2}{\varepsilon_p} \tag{5}$$

where $c_{\mu f}$ (=0.09) is a constant, k ($k = k_p + k_t$) is the turbulent kinetic energy, k_p is the turbulent kinetic energy of eddies in the production range, k_t is the turbulent kinetic energy of eddies in the dissipation range, and ε_p is the transfer rate of turbulent kinetic energy from the production range to the dissipation range.

Transport equations for the turbulent kinetic energies for the multiple-time-scale turbulence model are given as:

$$u \frac{\partial k_p}{\partial x} + v \frac{\partial k_p}{\partial y} - \frac{\partial}{\partial y} [(\nu + \frac{\nu_t}{\sigma_{kp}}) \frac{\partial k_p}{\partial y}] = Pr - \varepsilon_p \tag{6}$$

$$u \frac{\partial k_t}{\partial x} + v \frac{\partial k_t}{\partial y} - \frac{\partial}{\partial y} [(\nu + \frac{\nu_t}{\sigma_{kt}}) \frac{\partial k_t}{\partial y}] = \varepsilon_p - \varepsilon_t \tag{7}$$

where Pr is the production rate of turbulent kinetic energy, ε_t is the dissipation rate of the turbulent kinetic energy, and σ_{kp} and σ_{kt} are the turbulent Prandtl numbers for the turbulent kinetic energy equations.

The convection-diffusion equations for the energy transfer rate and the dissipation rate are given as:

$$u \frac{\partial \varepsilon_p}{\partial x} + v \frac{\partial \varepsilon_p}{\partial y} - \frac{\partial}{\partial y} \left[\left(\nu + \frac{\nu_t}{\sigma_{\varepsilon p}} \right) \frac{\partial \varepsilon_p}{\partial y} \right] = c_{p1} \frac{Pr^2}{k_p} + c_{p2} \frac{Pr \varepsilon_p}{k_p} - c_{p3} \frac{\varepsilon_p^2}{k_p} \quad (8)$$

$$u \frac{\partial \varepsilon_t}{\partial x} + v \frac{\partial \varepsilon_t}{\partial y} - \frac{\partial}{\partial y} \left[\left(\nu + \frac{\nu_t}{\sigma_{\varepsilon t}} \right) \frac{\partial \varepsilon_t}{\partial y} \right] = c_{t1} \frac{\varepsilon_p^2}{k_t} + c_{t2} \frac{\varepsilon_p \varepsilon_t}{k_t} - c_{t3} \frac{\varepsilon_t^2}{k_t} \quad (9)$$

where $c_{p\ell}$ ($\ell = 1,3$) and $c_{t\ell}$ ($\ell = 1,3$) are the turbulence model constants, and $\sigma_{\varepsilon p}$ and $\sigma_{\varepsilon t}$ are the turbulent Prandtl numbers for the energy transfer rate and the energy dissipation rate equations, respectively. The turbulence model constants are given as: $\sigma_{kp} = 0.75$, $\sigma_{\varepsilon p} = 1.15$, $\sigma_{kt} = 0.75$, $\sigma_{\varepsilon t} = 1.15$, $c_{p1} = 0.21$, $c_{p2} = 1.24$, $c_{p3} = 1.84$, $c_{t1} = 0.29$, $c_{t2} = 1.28$, and $c_{t3} = 1.66$ [11].

WALL FUNCTION BOUNDARY CONDITIONS

The near wall boundary conditions for k_p, k_t, ε_p, and ε_t were obtained from the standard wall function method. Detailed derivation of the wall function boundary conditions for the multiple-time-scale turbulence model can be found in Reference 11. These are given as,

$$\tau_w = - \left[\rho \kappa c_\mu^{1/4} k^{1/2} / \ln(Ey^+) \right] u \quad (10)$$

$$k = c_\mu^{-1/2} \tau_w / \rho \quad (11)$$

$$\varepsilon = \frac{1}{\kappa y} c_\mu^{3/4} k^{3/2} \quad (12)$$

$$\frac{k_t}{k_p} = \frac{\kappa^2}{\sigma_{\varepsilon p} c_\mu^{1/2} (c_{p3} - c_{p1} - c_{p2})} - 1 \quad (13)$$

$$\frac{\varepsilon_t}{\varepsilon_p} = 1 \quad . \quad (14)$$

COMPUTATIONAL RESULTS

The finite element computational procedure, as related to the two-layer approach, is described briefly below.

The governing differential equations were solved on the physical domain using physical dimensions. The wall shearing stress to be used in equations (1), (11), and (12) has been obtained by using equation (10). Alternatively, the wall shearing stress could have been computed by using the standard definition given as,

$$\tau_w = \mu \left[\frac{\partial u}{\partial y}\right]_{y=0} . \qquad (15)$$

Equation (15) is valid at and very close to the wall where the molecular viscosity dominates over the turbulent eddy viscosity. However, an accurate evaluation of the velocity gradient at the wall may require a significant number of grid points inside the near-wall layer. Furthermore, the turbulent kinetic energies, the energy transfer rate, and the dissipation rate were computed using the standard wall function method. Therefore, equation (10) has been preferred over equation (15) for the two-layer model presented herein.

All the governing differential equations and the wall function boundary conditions are nonlinearly coupled with each other; thus, the system of equations, including the wall function boundary conditions, have been solved iteratively until the prescribed convergence criterion was satisfied. A direct (Picard) iteration method has been used to solve the system of equations [10]. Details on the finite element method for turbulent flows can be found in Reference 10.

The initial condition data for velocity, turbulent kinetic energy, and dissipation rate were obtained from experimental data. The initial condition data for the ratios of k_p/k_t and $\varepsilon_p/\varepsilon_t$ were obtained by interpolating the near wall values and the free stream values of these ratios, respectively [11]. The wall function boundary conditions, equations (10) through (14), were used at the near wall boundary for the turbulence equations; and the vanishing gradient boundary condition was used at the outer edge of the computational domain for both the flow equations and the turbulence equations. Whenever necessary, the values of 1.225 kg/m^3 and 0.17854 x 10^{-4} kg/m-sec were used for density and molecular viscosity, respectively.

1. A Wall Jet Issuing Into a Moving Stream

The configuration of the wall jet flow considered herein can be found in References 10 and 18, and the experimental data for the flow can be found in Reference 18.

Input data used in computation of the flow were obtained directly and/or by curve-fitting the experimental data [10,18]. The transverse computational domain of the near-wall layer extended from the wall (y = 0 m) to y = 0.002 m; and that of the outer layer extended from y = 0.002 m to y = 0.08 m. The computational domain in

the flow direction extended from x = 0.5532 m (x/b = 82.2, where b is the jet slot width) to x = 1.6892 m (x/b = 251). Two different discretizations have been used in the present study. In the first case, the near-wall layer has been discretized by using 20 grids (10 equally space quadratic elements); and in the second case, two grid points (1 quadratic element) have been allocated in the near-wall layer. For both of the cases, the transverse domain in the outer layer has been discretized by 45 unequally spaced quadratic elements, and the flow direction domain has been discretized by 1135 line-steps. For both of the cases, an average of 12 iterations was required for each line-step to obtain convergent solutions. This number of iterations was found to be the same as the one given in the previous study [11], in which the standard wall function method had also been used for the flow equations at the near wall boundary.

The computational results of the flow development along the downstream direction, obtained by using the two-layer model, are compared with experimental data as well as those obtained by using the standard wall funciton method in Figure 3(a). The velocity, turbulent kinetic energy, and Reynolds stress at the far downstream location (x/b = 251) are shown in Figures 3(b); and the computed mean normal velocity profiles at the same downstream location are shown in Figure 3(c).

It can be seen in Figures 3(a) and 3(b) that the computational results for the tangential mean velocity and the turbulence quantities obtained by using the two-layer model are almost the same as those obtained by using the standard wall function method. However, the mean normal velocity obtained by using the two-layer model was slightly different from the one obtained by using the wall function method [Fig. 3(c)]. For the wall-jet flow, the characteristic mean tangential velocity was a few orders of magnitude greater than that of the mean normal velocity, hence, the mean tangential velocity and the turbulence quantities were not significantly influenced by the mean normal velocity.

It was found that the number of elements used to cover the near-wall layer did not exhibit significant influence on the converged solutions for all of the turbulent flow variables, and that the grid independent solution has been obtained with as small as two grid points (1 quadratic element) in the near wall layer.

2. Wake-Boundary Layer Interaction Flows

The configuration and the experimental data of the weakly coupled wake-boundary layer interaction flow considered herein can be found in Reference 19.

The transverse domain of the near-wall layer extended from the wall (y = 0 m) to y - 0.002 m; and that of the outer layer extended from y = 0.002 m to y = 0.12 m in the free stream region. The computational domain in the flow direction extended from x = 0.2 m (x/d = 20, where d is the diameter of the cylinder submerged in the boundary layer flow) to x = 0.86 m (x/d = 86). Two different discretizations have been used for the near-wall layer, the details of which are the same as in the previous wall-jet case. The transverse domain in the outer layer has been discretized by using 45 unequally spaced quadratic elements, and the flow direction domain has been discretized by using 825 line steps. Approximately 10 iterations were required for each line-step for all of the cases, including the case of using the wall function method.

The velocity, turbulent kinetic energy, and Reynolds stress at the far downstream location (x/d = 86) obtained by using the two-layer model are compared with

experimental data as well as those obtained by using the wall function method in Figures 4(a), and the computed mean normal velocity profiles at the same downstream location are shown in Figure 3(b). Again, the computational results for the tangential mean velocity and the turbulence quantities obtained by using the two-layer model were almost identical to those obtained by using the wall function method [Fig. 4(a). The mean normal velocity obtained by using the two-layer model was slightly different from the one obtained by using the wall function method [Fig. 4(b)]. As in the wall-jet case, the mean tangential velocity and the turbulence quantities were not significantly influenced by the mean normal velocity, and the grid independent solutions were obtained with as small as two grid points inside the near-wall layer.

CONCLUSIONS AND DISCUSSION

A two-layer multiple-time-scale turbulence model and grid independence study for turbulent boundary layer flows have been presented in this report. In the two-layer model, the computational domain for the conservation of mass equation and the mean momentum equation has been located at the wall where no slip boundary condition could be specified. Therefore, the conservation of mass constraint could have been satisfied more rigorously with the two-layer model than with the standard wall function method.

The mean normal velocity obtained by using the two-layer model was slightly different from the one obtained by using the standard wall function method. However, the tangential mean velocity and the turbulence quantities were not influenced significantly by the slight difference in the mean normal velocity. Hence, it was found that the performance of the turbulence model has not been masked by use of the wall function method for these example flow cases.

In the present finite element computation of the turbulent boundary layer flows, the grid independent solution has been obtained with only two grid points (1 quadratic element) inside the near-wall layer. In finite difference computations, it is usually known that at least eight grid points are required inside the near-wall layer for the simplest class two-layer models [1]. The required number of iterations to obtain convergent solutions was not increased by the use of the two-layer model compared with that of using the wall function method. To summarize, the two-layer model turned out to be more advantageous over the wall function method in finite element computation of turbulent boundary layer flows.

REFERENCES

1. Launder, B. E.: Numerical Comparison of Convective Heat Transfer in Complex Turbulent Flows: Time to Abandon Wall Functions? Int. J. Heat and Mass Transfer, Vol. 27, No. 9, 1984, pp. 1485-1491.

2. Gorski, J. J.: A New Near-Wall Formulation for the k-ε Equations of Turbulence. AIAA-86-0556, AIAA 24th Aerospace Sciences Meeting, Reno, NV, 1986.

3. Chen, H. C. and Patel, V. C.: Practical Near-Wall Turbulence Models for Complex Flows Including Separation. AIAA-87-1300, AIAA 25th Aerospace Sciences Meeting, Reno, NV, 1987.

4. Amano, R. S.: Development of a Turbulence Near-Wall Model and Its Application to Separated and Reattached Flows. Numerical Heat Transfer, Vol. 7, 1984, pp. 59-75.

5. Amano, R. S.: A Study of Turbulent Flow Downstream of an Abrupt Pipe Expansion. J. AIAA, Vol. 21, No. 10, 1983, pp. 1400-1405.

6. Hanjalic, K. and Launder, B. E.: Contribution Towards a Reynolds-Stress Closure for Low-Reynolds-Number Turbulence. J. Fluid Mechanics, Vol. 74, Part 4, 1976, pp. 593-610.

7. Patel, V. C., Rodi, W., and Scheuerer, G.: Turbulence Models for Near Wall and Low Reynolds Number Flows: A Review. J. AIAA, Vol. 23, 1985, pp. 1308-1319.

8. Tennekes, H. and Lumley, J. L.: A First Course in Turbulence. The MIT Press, MA, 1972.

9. Thomas, C. E., Morgan, K., and Taylor, C.: A Finite Element Analysis of Flow Over a Backward Facing Step. Computers and Fluids, Vol, 9, 1981, pp. 265-278.

10. Kim, S.-W. and Chen, Y.-S.: A Finite Element Computation of Turbulent Boundary Layer Flows with an Algebraic Stress Turbulence Model. To appear in J. Computer Methods in Applied Mechanics and Engineering, 1987.

11. Kim, S.-W. and Chen, C.-P.: A Multiple-Time-Scale Turbulence Model Based on Variable Partitioning of the Turbulent Kinetic Energy Spectrum. AIAA-88-0221, AIAA 26th Aerospace Sciences Meeting, Reno, NV, 1988. Also available as NASA CR, in print, 1987.

12. Benim, A. C. and Zinser, W.: Investigation Into the Finite Element Analysis of Confined Turbulent Flows Using a k-ε Model of Turbulence. Computer Methods in Applied Mechanics and Engineering, Vol. 51, 1985, pp. 507-523.

13. Hutton, A. G. and Smith, R. M.: On the Finite Element Simulation of Incompressible Turbulent Flow in General Two-Dimensional Geometries. C. Taylor and B. A. Schrefler, Editors, Numerical Methods in Laminar and Turbulent Flows, Pineridge Press, 1981.

14. Patankar, S. V.: Numerical Heat Transfer and Fluid Flow. McGraw-Hill, New York, 1980.

15. Kleinstein, G.: Generalized Law of the Wall and Eddy Viscosity Model for Wall Boundary Layer. J. AIAA, Vol. 5, No. 8, 1967, pp. 1402-1407.

16. Klebanoff, P. S.: Characteristics of Turbulence in a Boundary Layer with Zero Pressure Gradient. NACA CR-1247, 1954.

17. Laufer, J.: Investigation of Turbulent Flow in a Two-Dimensional Channel. NACA CR-1053, 1949.

18. Irwin, H. P. A. H.: Measurements in a Self-Preserving Plane Wall Jet in a Positive Pressure Gradient. J. Fluid Mechanics, Vol. 61, 1973, pp. 33-63.

19. Tsiolakis, E. P., Krause, E., and Muller, U. R.: Turbulent Boundary Layer-Wake Interaction. In Turbulent Shear Flows, Vol. 4, L. J. S. Bradbury, F. Durst, B. E. Launder, F. W. Schmidt, and J. H. Whitelaw, Editors, Springer-Verlag, New York, 1983.

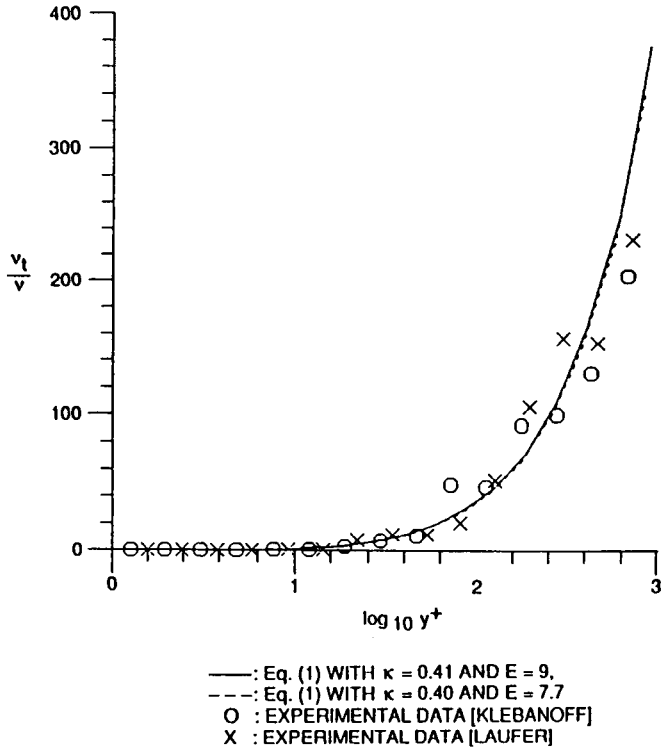

Figure 1. Effective turbulent eddy viscosity.

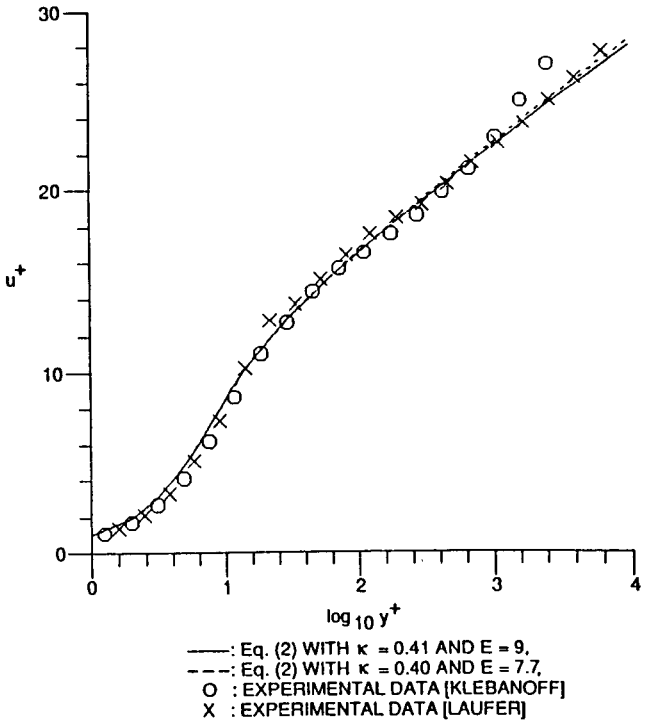

Figure 2. Logarithmic velocity profiles.

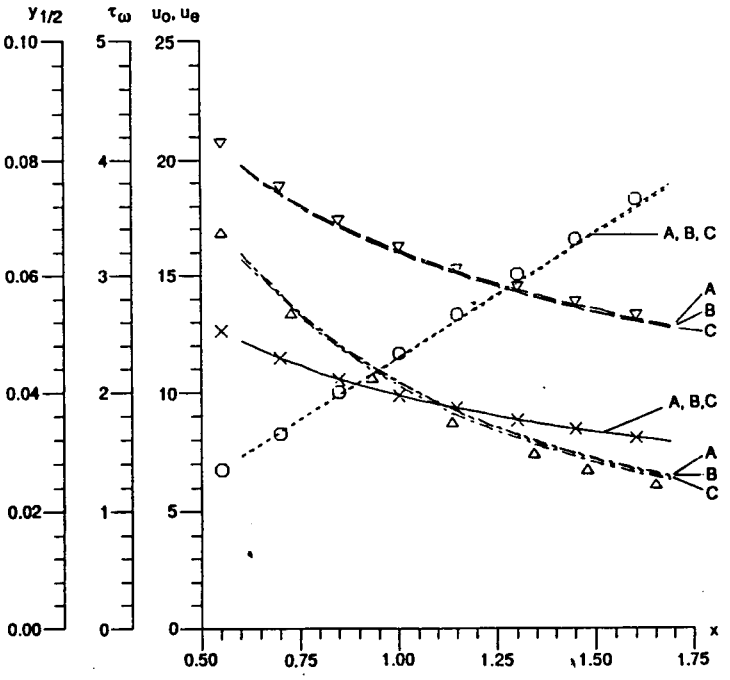

---, ——, — — —, — · —, ·····: COMPUT. MAX. EXCESS VELOCITY (u_0), EXTERNAL VELOCITY (u_e), WALL SHEARING STRESS (τ_ω), AND LENGTH SCALE ($y_{1/2}$), RESPECTIVELY; Δ, X, Δ, O: EXP'T u_0, u_e, τ_ω, $y_{1/2}$, RESPECTIVELY; A, B: 20 GRIDS (10 ELEMENTS) AND 2 GRIDS (1 ELEMENT) INSIDE THE NEAR-WALL LAYER, RESPECTIVELY; C: WALL FUNCTION METHOD.

Figure 3(a). Development of the wall-jet flow along the flow direction.

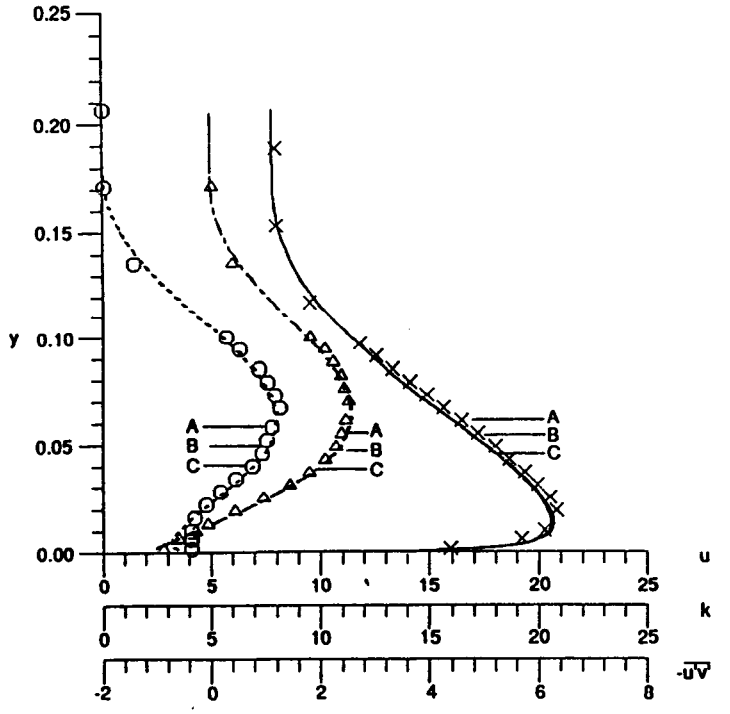

——, ·····, — · —, — · · — : COMPUT. RESULTS FOR VELOCITY (u), TURBULENT KINETIC ENERGY (k), AND REYNOLDS STRESS ($-\overline{uv}$), RESPECTIVELY; X, O, Δ: EXP'T DATA FOR u, k, $-\overline{uv}$, RESPECTIVELY; A, B : 20 GRIDS (10 ELEMENTS) AND 2 GRIDS (1 ELEMENT) INSIDE THE NEAR-WALL LAYER, RESPECTIVELY; C: WALL FUNCTION METHOD.

Figure 3(b). Velocity, turbulent kinetic energy, and Reynolds stress of the wall-jet flow at x = 1.6882 m.

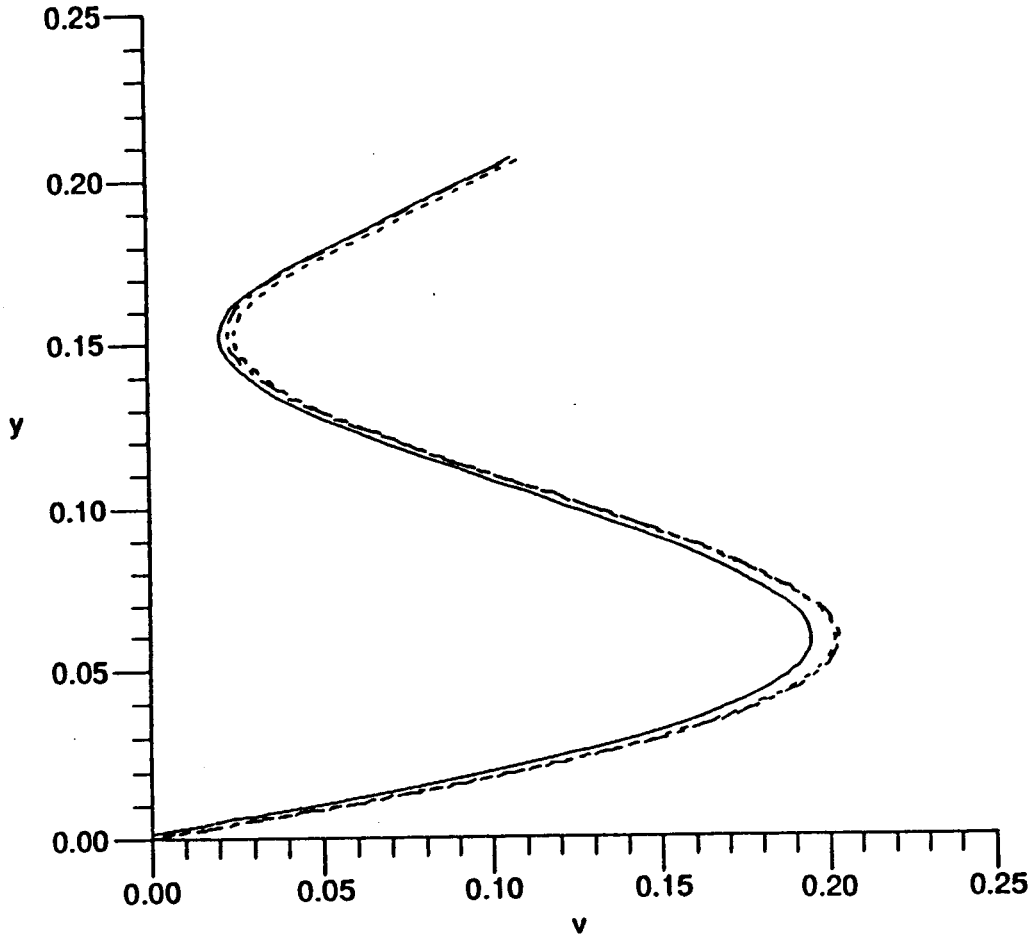

Figure 3(c). Normal velocity profile of the wall-jet flow at x = 1.6882 m.

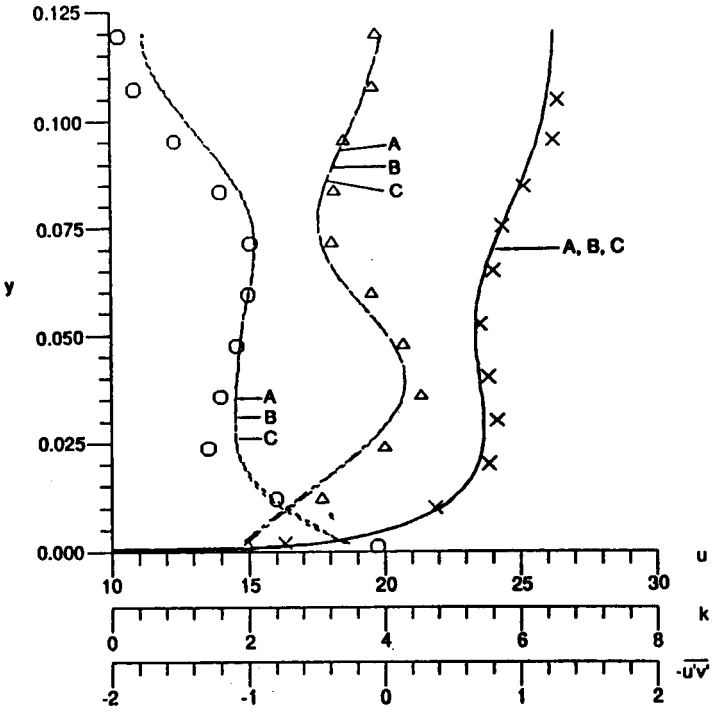

Figure 4(a). Velocity, turbulent kinetic energy, and Reynolds stress for the wake-boundary layer interaction flow, at x = 0.86 m. [Notations are the same as in Figure 3(b).]

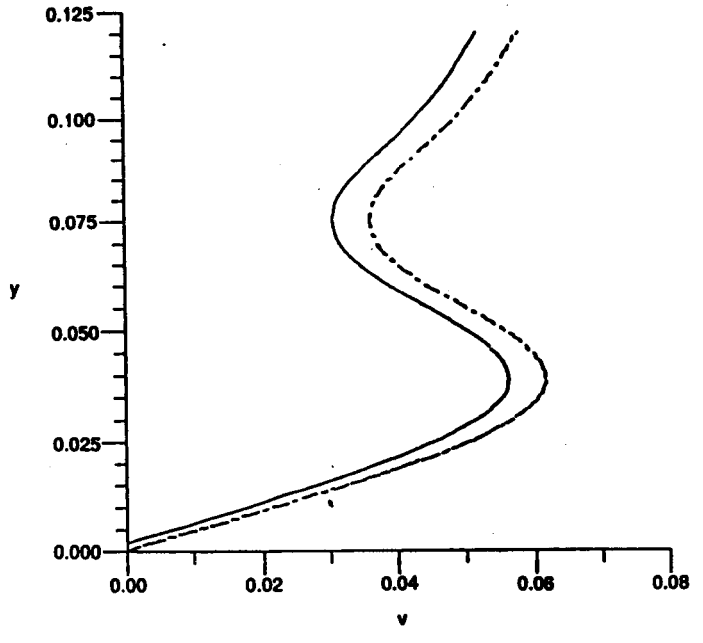

Figure 4(b). Normal velocity profile for the wake-boundary layer interaction flow at x = 0.86 m. [Notations are the same as in Figure 3(c).]

☆U.S. GOVERNMENT PRINTING OFFICE: 1989 - 631-056/00129

TECHNICAL REPORT STANDARD TITLE PAGE

1. REPORT NO.	2. GOVERNMENT ACCESSION NO.	3. RECIPIENT'S CATALOG NO.
NASA CR- 183653		

4. TITLE AND SUBTITLE

A Two-Layer Multiple-Time-Scale Turbulence Model and Grid Independence Study

5. REPORT DATE March 1989

6. PERFORMING ORGANIZATION CODE ES42

7. AUTHOR(S) S.-W. Kim* and C. -P. Chen**

8. PERFORMING ORGANIZATION REPORT #

9. PERFORMING ORGANIZATION NAME AND ADDRESS

George C. Marshall Space Flight Center
Marshall Space Flight Center, Alabama 35812

10. WORK UNIT NO.

11. CONTRACT OR GRANT NO. NAS8-35918

13. TYPE OF REPORT & PERIOD COVERED Contractor Report

12. SPONSORING AGENCY NAME AND ADDRESS

National Aeronautics and Space Administration
Washington, D.C. 20546

14. SPONSORING AGENCY CODE

15. SUPPLEMENTARY NOTES Prepared for the Fluid Dynamics Branch, Space Science Laboratory
Technical Monitor: N. C. Costes

*Universities Space Research Association
**Department of Mechanical Engineering, UAH, Huntsville, Alabama 35899.

16. ABSTRACT

A two-layer multiple-time-scale turbulence model is presented in this report. The near-wall model is based on the classical Kolmogorov-Prandtl turbulence hypothesis and the semi-empirical logarithmic law of the wall. In the two-layer model presented herein, the computational domain of the conservation of mass equation and the mean momentum equation penetrated up to the wall, where no slip boundary condition has been prescribed; and the near wall boundary of the turbulence equations has been located at the fully turbulent region, yet very close to the wall, where the standard wall function method has been applied. Thus, the conservation of mass constraint can be satisfied more rigorously in the two-layer model than in the standard wall function method. In most of the two-layer turbulence models, the number of grid points to be used inside the near-wall layer posed the issue of computational efficiency. The present finite element computational results showed that the grid independent solutions were obtained with as small as two grid points, i.e., one quadratic element, inside the near-wall layer. Comparison of the computational results obtained by using the two-layer model and those obtained by using the wall function method is also presented.

17. KEY WORDS	18. DISTRIBUTION STATEMENT
Turbulence Model, Computational, Fluid, High Reynolds Number Flow, Finite Element	Unclassified – Unlimited E. Tandberg-Hanssen Director, Space Science Laboratory

19. SECURITY CLASSIF. (of this report)	20. SECURITY CLASSIF. (of this page)	21. NO. OF PAGES	22. PRICE
Unclassified	Unclassified	17	NTIS